



Tricritical point in ferroelastic ammonium titanyl fluoride: NMR study

V.Ya. Kavun^a, S.G. Kozlova^{b,*}, N.M Laptash^a, I.A. Tkachenko^a, S.P Gabuda^b

^a Institute of Chemistry, FEB RAS, Ave. Stoletiya, 159, 690022 Vladivostok, Russia

^b Nikolaev Institute of Inorganic Chemistry, SB RAS, Ave. Lavrenteva, 3, 630090 Novosibirsk, Russia

ARTICLE INFO

Article history:

Received 28 March 2010

Received in revised form

12 July 2010

Accepted 17 July 2010

Available online 24 July 2010

Keywords:

Ferroelastic phase transitions

Jahn–Teller effect

Titanyl fluoride complex

¹⁹F NMR

Anisotropic rotation

Tricritical point

ABSTRACT

Ionic mobility and phase transitions in ammonium titanyl pentafluoride $(\text{NH}_4)_3\text{TiOF}_5$ were studied using the ¹⁹F and ¹H NMR data. The high-temperature phase (I) is characterized by spherically symmetric (isotropic) reorientation of $[\text{TiOF}_5]^{3-}$ anions and by uniaxial reorientation of these anions in the ferroelastic phase II. A previously unknown second-order phase transition to the low-temperature modification $(\text{NH}_4)_3\text{TiOF}_5(\text{III})$ was found at 205 K. The transition is accompanied by hindering of uniaxial rotations of $[\text{TiOF}_5]^{3-}$ anions and by noticeable change of ¹⁹F magnetic shielding tensor associated with the influence of pseudo-Jahn–Teller effect. A pressure-induced tricritical point with coordinates $p_{\text{TCR}} \approx 2$ kbar and $T_{\text{TCR}} \approx 170$ K is estimated on the base of ¹⁹F NMR chemical shift data, and previously studied p – T diagram of $(\text{NH}_4)_3\text{TiOF}_5$.

© 2010 Elsevier Inc. All rights reserved.

1. Introduction

Complex titanyl fluorides belong to a new family of coordinate compounds of titanile. Among them, potassium titanyl pentafluoride, K_3TiOF_5 , is both ferroelectric and ferroelastic below 490 K [1]. Ferroelastic phase transitions in ammonium titanyl pentafluoride complex $(\text{NH}_4)_3\text{TiOF}_5$ was found at $T_1 = 264.7 \pm 0.1$ K with the entropy change $\Delta S = \sim R \ln 8$ [2]. In the p – T diagram of this complex four phases and two triple points were found below 300 K and 5 kbar [2]. From a linear extrapolation of low-temperature high-pressure data to $p = 1$ bar a low-temperature phase transition at nearly ~ 120 K was predicted. However, the scanning calorimetric study [2] did not discover any thermal anomalies of $(\text{NH}_4)_3\text{TiOF}_5$ between T_1 and ~ 80 K, and the structural mechanism of the phase transitions has not been studied.

The crystal structure of high-temperature (paraelectric) phase of $(\text{NH}_4)_3\text{TiOF}_5$ belongs to the family of elpasolite, space group $Fm\bar{3}m$; $a = 9.113$ Å, $Z = 4$ [2]. The asymmetric titanyl pentafluoride ions (Fig. 1) occupy the 4(a) position of the O_h point symmetry, while the ammonium ions occupy 4(b) and 8(c) positions. It was supposed that F and O atoms in the paraelectric phase of $(\text{NH}_4)_3\text{TiOF}_5$ were distributed uniformly over the positions of perfect octahedrons. Here we show that isotropic reorientation of $[\text{TiOF}_5]^{3-}$ anions takes place in this case. The previously unknown first-order phase transition is revealed at 205 K. We also studied the variations of internal mobility

under the phase transitions, order–disorder phenomena and related electronic structure changes in $(\text{NH}_4)_3\text{TiOF}_5$ using the ¹⁹F and ¹H NMR solid-state spectroscopy and the density functional theory (DFT) calculations. The low-temperature phase transition is shown to be caused by hindering of uniaxial rotation of $[\text{TiOF}_5]^{3-}$ anions and symmetry lowering due to pseudo-degeneration of the electronic basic state resulting in the second-order Jahn–Teller effect.

2. Experimental

Ammonium oxofluotitanate $(\text{NH}_4)_3\text{TiOF}_5$ was synthesized in the form of well-shaped octahedral single crystals as a result of the ammoniac hydrolysis of the $(\text{NH}_4)_2\text{TiF}_6$ hot aqueous solution in the excess of NH_4F according to the original method described in [3]. The obtained crystals had dimensions of ~ 5 μm at fast crystallisation and up to ~ 40 μm at slow evaporation. According to IR spectroscopy data, the samples did not contain hydroxide ions within the detection limits (10^{-4} at%).

The ¹⁹F and ¹H NMR spectra were recorded using the spectrometers Bruker AV-300 (at the Larmor frequency $\nu_L = 282.404$ and 300.0 MHz), and Bruker SWL 3-100 ($\nu_L = 84.66$ MHz). The temperature varied in a stepwise manner between 150 and 360 K, the accuracy of temperature stabilization at each step was ± 3 K. A series of representative ¹⁹F and ¹H NMR spectra is shown in Fig. 2.

The calculation of the spectra second moments M_2 (mean-square width of the NMR spectrum in G^2 , see Fig. 3 and Table 1) has been carried out with the accuracy of $\sim 5\%$. The ¹⁹F NMR

* Corresponding author.

E-mail address: sgk@niic.nsc.ru (S.G. Kozlova).

chemical shifts were measured using C_6F_6 as a reference with $\sim 3\%$ accuracy. The ^{19}F NMR chemical shift of C_6F_6 relatively to an idealized fluorine ion $[F]^-$ is $\delta_{[F]^-}(C_6F_6) = 125$ ppm [4].

3. Results and data analysis

3.1. Intracrystalline ionic mobility in $(NH_4)_3TiOF_5$

Fig. 3 shows the temperature dependence of the second moment (M_2) for the ^{19}F NMR spectra of $(NH_4)_3TiOF_5$. Stepwise changes of M_2 are observed at temperatures of ~ 265 (PT_1) and

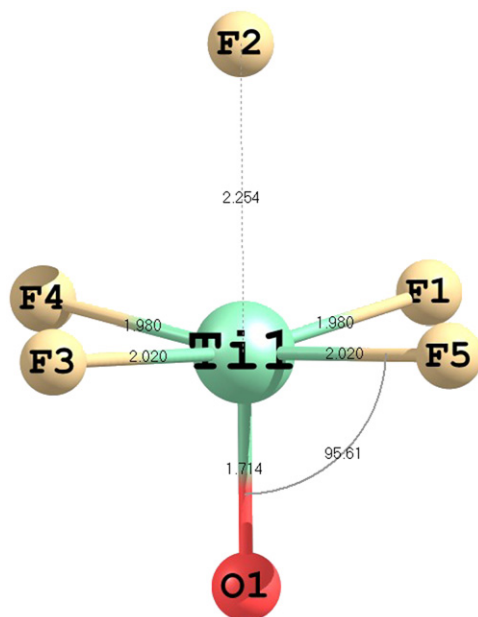


Fig. 1. Distorted structure of complex anion $[TiOF_5]^{3-}$ in phase $(NH_4)_3TiOF_5(III)$.

~ 205 K (PT_2). The first value is in close agreement with the temperature $T_1 = 264.7 \pm 0.1$ K of the first-order phase transition reported earlier [2]. The second stepwise change of M_2 observed at $T_2 \approx 205$ K can be related to the low-temperature phase transition PT_2 predicted previously in [2].

The uneven variations of $M_2(F)$ at PT_1 and PT_2 (Fig. 3) result in abrupt changes of structural ordering and intracrystalline ionic mobility accompanying the solid–solid phase transitions. According to the fundamentals of the NMR theory [5], the above intracrystalline ionic mobilities are represented by orientation diffusion of constituent molecular anions $[TiOF_5]^{3-}$ and cations $[NH_4]^+$ and fast proton exchange in the high-temperature phase I. In Table 1 the experimental M_2 data are juxtaposed with the expected ones calculated for different modes of intracrystalline mobility in different phases of $(NH_4)_3TiOF_5$.

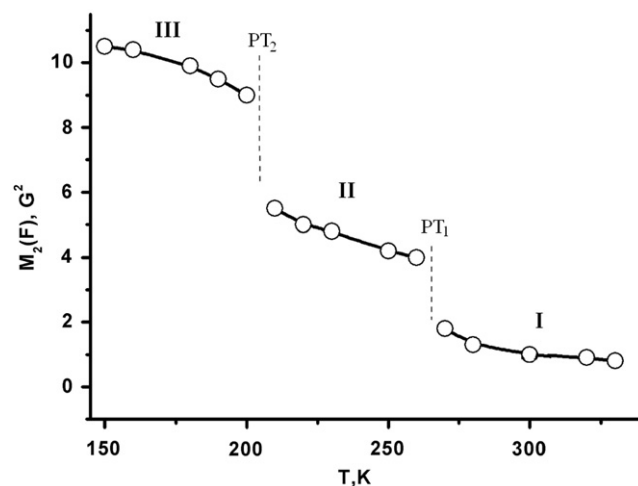


Fig. 3. Temperature dependence of the second moments of ^{19}F NMR spectra of $(NH_4)_3TiOF_5$ measured in the magnetic field of $B_0 = 21.140$ kG at the Larmor frequency $\nu_L = 84.66$ MHz.

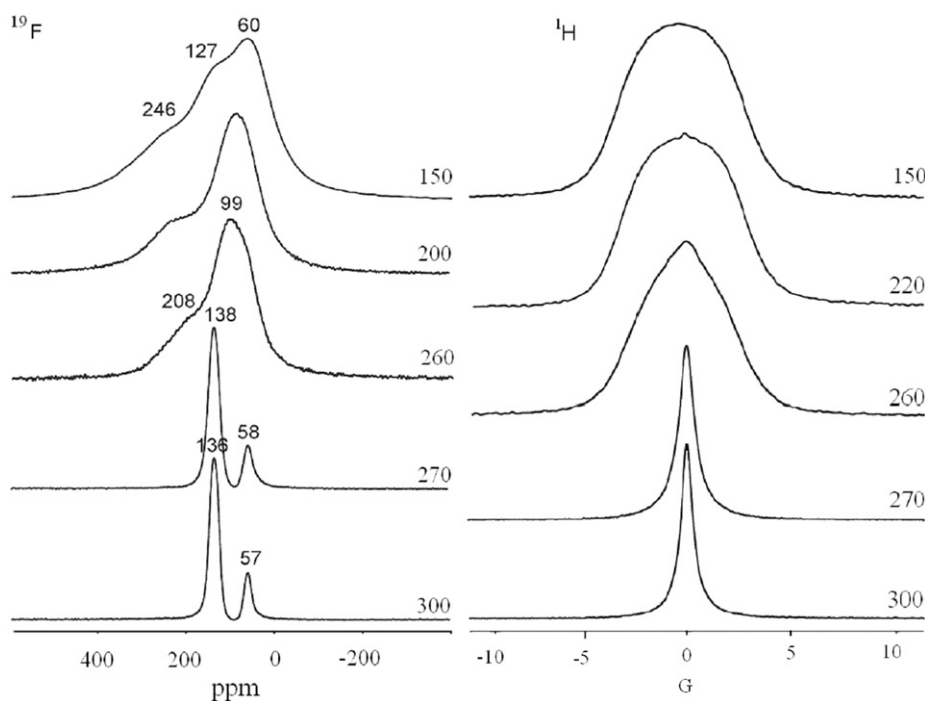


Fig. 2. Temperature variations of ^{19}F and 1H NMR spectra of $(NH_4)_3TiOF_5$ recorded in the magnetic field of $B_0 = 70.5$ kG at the Larmor frequencies $\nu_L = 282.404$ and 300.0 MHz.

Table 1
Measured and calculated mean-square widths of ^{19}F and ^1H NMR spectra in different phases of $(\text{NH}_4)_3\text{TiOF}_5$.

Phase	$M_2(\text{F}), \text{G}^2$		$M_2(\text{H}), \text{G}^2$	
	Experimental	Calculated (mobility mode)	Experimental	Calculated (mobility mode)
I (above 265 K)	1.8–1.0	2.08 ($[\text{TiOF}_5]^{3-}$ anion isotropic reorientation)	~1–0	0 (proton exchange/translation diffusion)
II (between 265 and 205 K)	4.0–5.5	6.6 ($[\text{TiOF}_5]^{3-}$ anion uniaxial reorientation)	5.0–5.5	7.5 ($[\text{NH}_4]^+$ cation isotropic reorientation)
III (below 205 K)	9.0–10.5	8.1 (rigid fluorine sublattice)	6.0–8.5	7.5 ($[\text{NH}_4]^+$ cation isotropic reorientation)

3.2. ^{19}F NMR chemical shifts and the electronic structure of $[\text{TiOF}_5]^{3-}$ ion

Remarkably, ^{19}F NMR spectra of $(\text{NH}_4)_3\text{TiOF}_5$ has a specific two-component structure with the amplitude ratio 4:1 (Fig. 2) corresponding to that of fluorine atoms in *cis*- and *trans*-positions relative to O^{2-} ion in complexes $[\text{TiOF}_5]^{3-}$. The latter indicates the absence of the intramolecular exchange $\text{F}_{\text{cis}} \leftrightarrow \text{F}_{\text{trans}}$. One should also mention that the above fact excludes the possibility of the exchange $\text{F} \leftrightarrow \text{O}$ since it inevitably results in the exchange $\text{F}_{\text{cis}} \leftrightarrow \text{F}_{\text{trans}}$. To sum it up, the intracrystalline mobility in $(\text{NH}_4)_3\text{TiOF}_5$ is represented only by isotropic (in phase I) or single-axis (in phase II) rotational dynamics of structurally rigid particles $[\text{TiOF}_5]^{3-}$ with the exception of a substantial contribution from intramolecular dynamic processes of the Berry pseudorotation type [4].

The obtained result indicates that a multi-particle interaction in complex ions $[\text{TiOF}_5]^{3-}$ can be approximated by the sum of pair-wise interactions Ti–O and Ti– F_{trans} and of the coordination interaction in the flat-square group $\text{Ti}(\text{F}_{\text{cis}})_4$. Since the value of chemical shift of ^{19}F NMR for F_{trans} does not virtually change at the temperature decrease from 300 K [$\delta_{\text{C}_6\text{F}_6}(\text{F}_{\text{trans}}) = 57$ ppm] down to 150 K [$\delta_{\text{C}_6\text{F}_6}(\text{F}_{\text{trans}}) = 60$ ppm], one can assume that the phase transitions PT_1 and PT_2 in $(\text{NH}_4)_3\text{TiOF}_5$ do not affect the Ti– F_{trans} interaction.

On the other hand, in the case of the F_{cis} atoms one can observe dramatic changes of the spectral bands ^{19}F NMR at both phase transitions (PT_1 and PT_2). In particular, the F_{cis} singlet band characterized at 300 K by the value of chemical shift [$\delta_{\text{C}_6\text{F}_6}(\text{F}_{\text{cis}}) = 136$ ppm] broadens significantly at the temperature decrease down to 260 K. The asymmetric shape of this band corresponds to the system with a single-axis anisotropy of the ^{19}F NMR [4,5] chemical shift tensor for F_{cis} characterized by parameters of $\delta_{\parallel}(\text{F}_{\text{cis}}) = 208$ ppm and $\delta_{\perp}(\text{F}_{\text{cis}}) = 99$ ppm (at $T = 260$ K in Fig. 1). For such a system with a single-axis anisotropy of the chemical shift one can calculate the isotropic average value of the ^{19}F NMR chemical shift of the F_{cis} atoms in the phase $(\text{NH}_4)_3\text{TiOF}_5(\text{II})$:

$$\langle \delta(\text{II}) \rangle = 1/3(\delta_{\parallel} + 2\delta_{\perp}) = 135 \text{ ppm}$$

The obtained value coincides with the experimental one for the ^{19}F NMR chemical shift of the F_{cis} atoms in the high-temperature phase $(\text{NH}_4)_3\text{TiOF}_5$ (I), where [$\delta_{\text{C}_6\text{F}_6}(\text{F}_{\text{cis}}) = 136$ ppm] at 300 K (Fig. 2). The result indicates to the absence of changes in the electronic structures of the complexes $[\text{TiOF}_5]^{3-}$ at transition from their isotropic reorientation in the high-temperature phase $(\text{NH}_4)_3\text{TiOF}_5$ (I) to the single-axis rotation in the phase $(\text{NH}_4)_3\text{TiOF}_5$ (II). The above conclusion corroborates the results of the analysis of M_2 (Table 1).

3.3. Variation of ^{19}F NMR chemical shift tensor at PT_2

It may be expected that retardation of a single-axis reorientation of the flat-square group $\text{Ti}(\text{F}_{\text{cis}})_4$ at the low-temperature phase transition PT_2 cannot affect the longitudinal value of ^{19}F

Table 2
Measured and calculated parameters of ^{19}F NMR chemical shift tensor in the distorted phase of $(\text{NH}_4)_3\text{TiOF}_5(\text{III})$.

F position	$\delta_x[\text{F}]^-$ (ppm)	$\delta_y[\text{F}]^-$ (ppm)	$\delta_z[\text{F}]^-$ (ppm)	$\delta_{\text{iso}}[\text{F}]^-$ (ppm)
F1($\text{F}_{\text{cis}1}$)	35	94	345	158
F3($\text{F}_{\text{cis}2}$)	23	73	310	136
F_{cis} (exp)	~70	127 ± 3	246 ± 3	~150

NMR chemical shift tensor $\delta_{\parallel}(\text{F}_{\text{cis}}) = 208$ ppm, because the rotation does not induce fluctuation of local magnetic fields when the reorientation axis and the direction of the magnetic field are parallel. However, in the experiment the largest component (z-component) of the ^{19}F NMR chemical shift of the F_{cis} atoms in the phase $(\text{NH}_4)_3\text{TiOF}_5(\text{III})$ appears to be equal to $\delta_z(\text{F}_{\text{cis}}) = 246$ ppm (at $T = 150$ K in Fig. 2). Since the above component is parallel to the axis C_4 of the complexes $[\text{TiOF}_5]^{3-}$, one can see that at the low-temperature phase transition there occurs an abrupt change of the chemical shift tensor resulting in the disparity $\delta_z(\text{F}_{\text{cis}}) \neq \delta_{\parallel}(\text{F}_{\text{cis}})$.

The second component of the ^{19}F NMR chemical shift tensor of the F_{cis} atoms in the phase $(\text{NH}_4)_3\text{TiOF}_5(\text{III})$ corresponds to the magnetic field orientation perpendicular both to the C_4 -axis and the direction of the bond Ti– F_{cis} . The numerical value of this component visible at $T = 150$ K (in Fig. 2) is equal to $\delta_y = 127$ ppm. The estimation for the value of the third component of the ^{19}F NMR chemical shift ($\delta_x \approx 70$ ppm) parallel to the bond Ti– F_{cis} can be made by using the relation:

$$\langle \delta(\text{III}) \rangle = 1/3(\delta_x + \delta_y + \delta_z)$$

In this case $\langle \delta(\text{III}) \rangle$ stands for a weight-average value of the ^{19}F NMR chemical shift of the spectrum obtained at 150 K—it was found to be equal approximately to $\langle \delta(\text{III}) \rangle \approx 150$ ppm. The obtained final experimental values of the components of the ^{19}F NMR chemical shift tensors of the atoms F_{cis} in the phase $(\text{NH}_4)_3\text{TiOF}_5(\text{III})$ are presented in Table 2.

The observed abrupt change of the chemical shift tensor at the low-temperature phase transition can be related to the influence of the Jahn–Teller pseudo-effect (or vibronic interaction) in the systems with the coordination type of interaction, whose typical representatives include barium titanate and other ferroelectrics of the perovskite structural type [6]. In the case of octahedral complexes $[\text{TiOF}_5]^{3-}$ the influence of vibronic interaction is accompanied by the lowering of their axial C_4 symmetry due to its instability relatively to the off-axial displacements of the central atom Ti^{4+} . Resulting acentric C_s structure shows the formation of two shorter and two longer bonds Ti– F_{cis} produced by the shift of the Ti^{4+} ion in the plane of four atoms F_{cis} (Fig. 1). One of this effect repercussions comprises an abrupt change of the ^{19}F NMR chemical shift tensor at the low-temperature phase transition PT_2 and, in particular, the transition from the value $\delta_{\parallel}(\text{F}_{\text{cis}}) = 208$ ppm for the phase II to the value $\delta_z(\text{F}_{\text{cis}}) = 246$ ppm for the phase III.

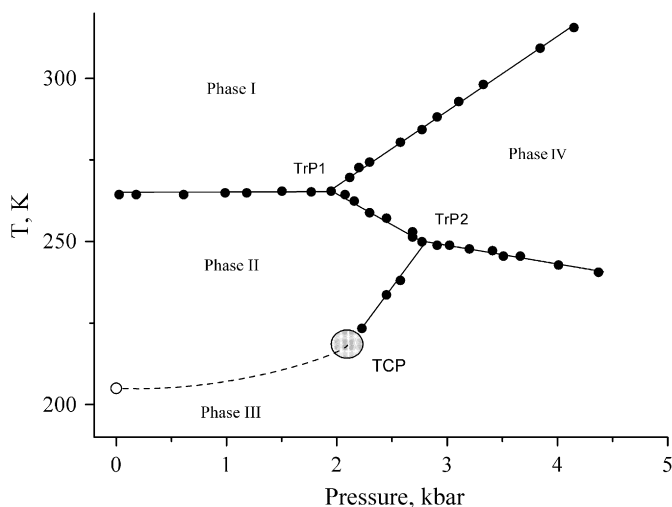


Fig. 4. Refined p - T phase diagram of $(\text{NH}_4)_3\text{TiOF}_5$. The experimental data of the previous work [2] and the present study are shown as (●) and (○), respectively; TCP is the estimated tricritical point. The dotted line indicates the boundary between the phase II and the low-temperature phase III.

3.4. DFT calculation of chemical shift tensor in $(\text{NH}_4)_3\text{TiOF}_5(\text{III})$

The numerical study of the chemical shift tensor of the free anion $[\text{TiOF}_5]^{3-}$ was performed on the basis of the density functional theory (DFT) with use of the software suite ADF-2008 [7], where the model Hamiltonians of the density functional were represented by the sum of the local density functional approximation (LDA) of Vosko et al. [8] and the generalized gradient functional GGA of Becke [9] and of Perdew [10]. Three-exponent Slater orbitals without the core potential were taken as basic wave functions (TZP/ADF-2008). The calculations of the ^{19}F NMR chemical shifts were conducted using generalized functionals and above mentioned wave functions, in accordance with the GIAO-DFT method to take into account all relativistic effects (ZORA method) [11–14]. The calculation results for the complex distorted structure (Fig. 1) are presented in Table 2. Juxtaposition of calculated and experimental data demonstrates a qualitative agreement between the calculated and measured parameters of the NMR chemical shifts.

4. Discussion and conclusion

According to a scanning calorimetric study [2], p - T diagram of $(\text{NH}_4)_3\text{TiOF}_5$ shows four phases and two triple points (TrP) of parameters $T_{1\text{trp}}=265.7$ K; $p_{1\text{trp}}=1.96$ kbar, and $T_{2\text{trp}}=249.2$ K; $p_{2\text{trp}}=2.91$ kbar (Fig. 4). From a linear extrapolation of low-temperature high-pressure data to $p=1$ bar a low-temperature phase transition was predicted at nearly ~ 120 K. However, the calorimetric study [2] did not discover any thermal anomalies of $(\text{NH}_4)_3\text{TiOF}_5$ between 265 and ~ 80 K.

The ^{19}F NMR data shown above confirm unambiguously the presence of the low-temperature phase transition PT_2 at $T \approx 205$ K. The characteristics of this phase transition, namely, the hindering of the uniaxial reorientation of $[\text{TiOF}_5]^{3-}$ anions and

accompanying change of ^{19}F NMR chemical shift tensors combined with the absence of thermal effects [2] might indicate its closeness to the second-order phase transition [15]. On the p - T diagram the solid line of the PT_2 phase transition can merge at elevated pressures with the high-pressure and low-temperature branch of phase diagram to show the pattern of lines of first-order phase transitions of $(\text{NH}_4)_3\text{TiOF}_5$ (Fig. 4). The junction point of two lines is the so-called tricritical point (TCP) observed in the most of ferroelectrics at elevated pressures [16,17]. The pressure value of the tricritical point in $(\text{NH}_4)_3\text{TiOF}_5$ can be estimated as close to $p_{\text{TCR}} \approx 2$ kbar and $T_{\text{TCR}} \approx 170$ K. The estimation is based mainly on previously studied p - T diagram of $(\text{NH}_4)_3\text{TiOF}_5$ [2] revealing noticeable low-temperature thermal anomalies above $p=2.25$ kbar (Fig. 4) with account of the above ^{19}F NMR solid-state data.

The phenomenon of tricritical point is related to the effect of competition of different interactions [17]. Vibronic interaction responsible for the ordering of $[\text{TiOF}_5]^{3-}$ anions in the studied system can compete with hydrogen bond $\text{N-H}\cdots\text{F}$ interaction of these anions with NH_4^+ in octahedral sites 4(b) of the initial $Fm\bar{3}m$ structure. According to ^1H NMR data (Fig. 2b and Table 1), H atoms are dynamically disordered in both II and III phases. However, the ordering in H-atom sublattice can be expected to occur in the high-pressure phase IV. If the arrangement of hydrogen atoms of NH_4^+ ions is ordered in the high-pressure Phase IV, the local symmetry C_4 of 4(b) sites must be lowered to the point symmetry of $\bar{4}$, and the probable space group symmetry will reduce to $I\bar{4}$ as is the case in structurally close systems of ammonium halogenides [18].

Acknowledgments

The study was supported by the Siberian Branch of RAS (Grant no. 100) and by the Russian Foundation for Basic Research (Grant no. 08-03-00826).

References

- [1] M. Fouad, J.P. Chaminade, J. Ravez, P. Hagenmuller, Rev. Chim. Miner. 24 (1987) 1–9.
- [2] I.N. Flerov, M.V. Gorev, V.D. Fokina, A.F. Bovina, N.M. Laptash, Phys. Solid State 46 (2004) 915–921.
- [3] N.M. Laptash, I.G. Maslennikova, T.A. Kaidalova, J. Fluorine Chem. 99 (1999) 133–137.
- [4] S.P. Gabuda, Yu.V. Gagarinsky, S.A. Polishchuk, NMR in Inorganic Fluorides, Atomic Energy Press (Atomizdat), Moscow, 1978 in Russian.
- [5] A. Abragam, Nuclear Magnetism, Oxford University Press, Oxford, 1960.
- [6] I.B. Bersuker, The Jahn–Teller Effect and Vibronic Interactions in Chemistry, Plenum, New York, 1982.
- [7] Amsterdam Density Functional (ADF) program, Release 2008.02, Vrije Universiteit, Amsterdam, The Netherlands, 2008.
- [8] S.H. Vosko, L. Wilk, M. Nusair, Can. J. Phys. 58 (1980) 1200–1211.
- [9] A.D. Becke, Phys. Rev. A 38 (1988) 3098–3100.
- [10] J.P. Perdew, Phys. Rev. B 33 (1986) 8822–8824.
- [11] E. van Lenthe, A.E. Ehlers, E.J. Baerends, J. Chem. Phys. 110 (1999) 8943–8953.
- [12] G. Schreckenbach, T. Ziegler, J. Phys. Chem. 99 (1995) 606–611.
- [13] G. Schreckenbach, T. Ziegler, Int. J. Quantum Chem. 61 (1997) 899–903.
- [14] G. Wolff, T. Ziegler, J. Chem. Phys. 109 (1998) 895–901.
- [15] A.Z. Patashinskii, V.L. Pokrovskii, Fluctuation Theory of Phase Transitions, Pergamon, Oxford, 1979.
- [16] V.H. Schmidt, A.B. Western, A.G. Baker, Phys. Rev. Lett. 37 (1976) 839–842.
- [17] V. Fridkin, Ferroelectrics 354 (2007) 259–264.
- [18] E.B. Amitin, Yu.A. Kovalevskaya, I.E. Paukov, K.S. Sukhovei, J. Eng. Phys. Thermophys. 39 (1980) 1381–1384.